

Learning to explore when mistakes are not allowed

Charly Pecqueux-Guézénec
Sorbonne Université, CNRS, ISIR
F-75005 Paris, France
pecqueuxguezénec@isir.upmc.fr

Stéphane Doncieux
Sorbonne Université, CNRS, ISIR
F-75005 Paris, France
doncieux@isir.upmc.fr

Nicolas Perrin-Gilbert
Sorbonne Université, CNRS, ISIR
F-75005 Paris, France
perrin@isir.upmc.fr

ABSTRACT

Goal-Conditioned Reinforcement Learning (GCRL) provides a versatile framework for developing unified controllers capable of handling wide ranges of tasks, exploring environments, and adapting behaviors. However, its reliance on trial-and-error poses challenges for real-world applications, as errors can result in costly and potentially damaging consequences. To address the need for safer learning, we propose a method that enables agents to learn goal-conditioned behaviors that explore without the risk of making harmful mistakes. Exploration without risks can seem paradoxical, but environment dynamics are often uniform in space, therefore a policy trained for safety without exploration purposes can still be exploited globally. Our proposed approach involves two distinct phases. First, during a pretraining phase, we employ safe reinforcement learning and distributional techniques to train a safety policy that actively tries to avoid failures in various situations. In the subsequent safe exploration phase, a goal-conditioned (GC) policy is learned while ensuring safety. To achieve this, we implement an action-selection mechanism leveraging the previously learned distributional safety critics to arbitrate between the safety policy and the GC policy, ensuring safe exploration by switching to the safety policy when needed. We evaluate our method in simulated environments and demonstrate that it not only provides substantial coverage of the goal space but also reduces the occurrence of mistakes to a minimum, in stark contrast to traditional GCRL approaches. Additionally, we conduct an ablation study and analyze failure modes, offering insights for future research directions.

KEYWORDS

Safe Exploration, Safe Reinforcement Learning, Goal-Conditioned Reinforcement Learning

1 INTRODUCTION

Goal-conditioned reinforcement learning (GCRL) provides bases to build a single robotic controller that can achieve a wide variety of tasks and adapt its behavior to its environment [6, 8, 10, 31]. GCRL methods have shown impressive performance on a wide variety of tasks, in simulation but also in the real world, essentially with manipulator robots [7, 28, 29]. In the case of manipulator robots, the action is often the desired position of the end effector. Then the agent strongly depends on primitives, facilitating exploration and avoiding safety problems.

However, moving towards fully autonomous agents, we would like to build robots that can explore their environment and discover new skills while staying out of danger. An example of such an ideal case would be a humanoid robot that does not fall while learning to move around in a new environment. Though it may seem contradictory at first glance, humans constantly explore new environments with the confidence that their balance and walking skills

will enable them to do it safely. Hikers, for instance, can navigate in unknown terrains with minor risks as their knowledge on how to avoid falling is general and applicable to diverse environments. Transposing these intuitions into formal vocabulary from viability theory [38], hikers know how to remain in viable states, even when they explore.

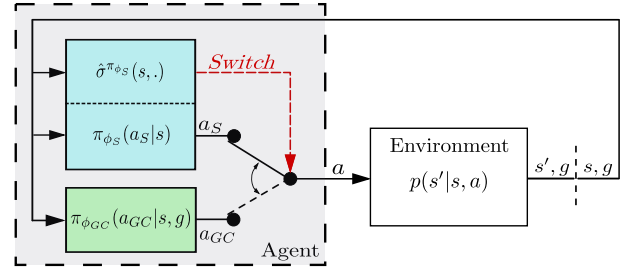


Figure 1: Action selection mechanism to guarantee safe exploration. The agent observes the current state s of the environment and the current goal g . The safety policy samples an action $a_S \sim \pi_{\phi_S}(\cdot | s)$ that must prevent future mistakes, while the goal-conditioned policy samples an action $a_{GC} \sim \pi_{\phi_{GC}}(\cdot | s, g)$ to go towards g . For each possibility, the function $\sigma^{\pi_{\phi_S}}$ estimates the level of confidence in the safety policy’s ability to avoid potential future errors. If it is too low, the safe action a_S is executed to keep the system safe. Otherwise, a_{GC} is executed, allowing the agent to explore.

We propose a safe exploration method that combines a goal-conditioned (GC) policy aiming to explore, discover and learn to cover a goal space of positions, and a safety policy aiming at maintaining the system in viable states. As the system dynamics are usually invariant in space and independent from the agent’s goals, the safety policy is defined independently from goals with the hope that it will be globally reliable. The method involves two distinct phases: a first phase of *pretraining* and a second phase of *safe exploration*. In the first phase, the safety policy is trained in simulation using safe reinforcement learning (safe RL) and distributional critics. In the second phase, the GC policy is trained. To avoid mistakes during exploration, an action-selection mechanism estimates the risk for future states to be unviable thanks to the distributional critics of the safety policy, then chooses which policy to execute at the current step. Obtaining theoretical results would depend on strong assumptions about the environment dynamics and near-perfect knowledge from the safety policy. Instead, our work focuses on empirically demonstrating that, in practice, an agent can learn to explore safely without making mistakes. Contrary to other approaches assuming to have access to instantaneous emergency actions [12, 37], we test our approach on two environments for which there exist states

that irreversibly lead to mistakes or failures: a goal-based version of CartPole and an environment based on the Skydio X2 drone from Mujoco Menagerie [35, 41]. In these environments, random actions or even zero actions lead to mistakes, which makes the conservation of safety quite challenging. To our knowledge, our approach is the only one that explicitly gathers safe RL and GCRL to perform safe exploration.

Our contributions are threefold:

- The design of a distributional safe RL framework to pre-train a safety policy that will prevent mistakes during the exploration phase.
- The design of an action selection mechanism to ensure safe exploration.
- The study of the key components of the method and failure modes to orient future research.

2 RELATED WORK

Safe Reinforcement Learning. Constrained optimal control methods allow to synthesize controllers with safety guarantees but they assume a perfect or at least partial knowledge of the system dynamics [3, 13, 23]. On the contrary, model-free safe reinforcement learning (safe RL) only assumes the system dynamics to be stochastic and markovian. Most safe RL methods aim at solving a Constrained Markov Decision Process (CMDP), which is built upon an analogy between rewards and constraints [1, 2, 9, 15, 17], as they formulate the constraint as a discounted cumulative objective, which is convenient from the RL point of view but not sufficient to satisfy persistent safety constraints along trajectories. To overcome this issue, some methods reformulate the critic target. For example, in [32], a safety critic allows to formulate the constraint in terms of failure probability [32]. Reachability-constrained RL (RCRL) [40] proposes to use a max operator in the safety critic target to discover the largest set of reachable states by the policy. In our work, we pre-train a safety policy using ingredients from RCRL and then use the critic in the safe exploration phase to decide when to switch from one policy to another. Also, since our goal is to prevent the worst-case scenario, we use quantile-based distributional reinforcement learning to train our safety policy [11, 34, 39].

Goal-conditioned RL. The standard RL framework addresses a single task, specified by the reward function. Goal-conditioned reinforcement learning (GCRL) provide bases to build a single robotic controller that is able to achieve a wide variety of tasks and adapt its behavior to its environment [10, 20, 31]. A goal can be a desired position for a given rigid body in the environment. In addition to being convenient for a robot user, it allows to learn from failed attempts. Indeed, an agent that has failed to reach a given desired goal has actually reached another accidentally. This feature can be exploited by relabelling methods, like Hindsight Experience Replay (HER), to learn a goal-conditioned policy from sparse rewards. In our experiments, we consider a sparse reward setting and combine Soft Actor-Critic (SAC) and HER to learn goal-conditioned policies [6, 18].

Learning diverse safe skills. Ha et al. have developed a method to learn safe locomotion in three directions for the Minitaur robot.

Although policy improvement over time leads to constraint satisfaction, reducing the need for human intervention for resets, the formalism does not explicitly enforce constraint satisfaction during exploration [17]. SASD on the other hand combines unsupervised skill discovery and safe RL to learn a richer set of skills, but still does not enforce safety during the exploration phase [22].

Safe exploration. Ladosz et al. identify two categories of safe exploration methods: those based on auxiliary reward and those based on human designer knowledge [25]. Auxiliary reward methods penalize the agent when it puts itself in danger. By definition, these methods incentivize the agent to avoid repeated mistakes and catastrophic behaviors, but do not constrain the exploration policy behavior directly. As a result, they reduce the occurrence of mistakes compared to baselines [21] or even improve learning [14, 27] but do not prevent them. In methods based on human designer knowledge, boundaries safe and unsafe states or behaviors are defined by the human designer. Most of these methods make strong assumptions about the environment or the agent behavior, which allows the use of baseline behaviors, human intervention, hand-crafted model or heuristics [16, 19, 30, 36]. A recent approach proposes a Meta-Algorithm for Safe Exploration (MASE) and provides theoretical guarantees on optimality and safety during exploration [37]. However, this approach assumes the agent has access to an emergency stop action that can reset the environment when no viable actions are available, an assumption that does not hold in general, and particularly not in our environments. In contrast, our focus is on environments where unviable states exist, and the agent must navigate within these constraints. Closer to us, Dalal et al. [12] use a pre-trained linearized constraint model and solve a quadratic program to project actions onto a feasible set during exploration. Their method, however, assumes access to a linearized model and that constraint violations can be avoided in a single step, which is not our case. Like us, Srinivasan et al. [32] propose two training phases. But they pre-train and then fine-tune a single policy, while we consider two different policies that are trained separately and, above all, do not share the same input. In our approach, the constraint function is used as an auxiliary reward signal for the safety policy, unlike other auxiliary reward methods where it influences the task-solving policy. Additionally, by making general assumptions about the environment’s structure, such as the uniformity in space of the dynamics, our method straddles both categories. Also, contrary to previously cited approaches, we explicitly merge GCRL with safe RL tools to build our safe exploration framework.

3 BACKGROUND

In this section, we introduce the notations and building blocks needed to develop our safe exploration method: RL and safe RL for learning the safety policy, goal-conditioned RL to achieve goals and distributional critics for risk-aware action selection during the safe exploration phase.

3.1 Reinforcement Learning formalism

An RL problem is described by a tuple $(\mathcal{S}, \mathcal{A}, p, p_0, r)$, called a Markov decision process (MDP), where \mathcal{S} is the state space, \mathcal{A} the action space, $p : \mathcal{S} \times \mathcal{A} \rightarrow \mathcal{P}(\mathcal{S})$ the transition function, $p_0 \in \mathcal{P}(\mathcal{S})$ the initial state probability distribution, $r : \mathcal{S} \times \mathcal{A} \rightarrow \mathbb{R}$

the reward function. The objective in RL is to obtain a policy $\pi : \mathcal{S} \rightarrow \mathcal{P}(\mathcal{A})$ that maximizes the expected sum of discounted rewards $\mathbb{E}_\pi \left[\sum_{t=0}^{+\infty} \gamma^t r(s_t, a_t) \right]$, where $\gamma \in [0, 1]$ is the discount factor [33].

3.2 Goal-conditioned RL formalism

Goal-conditioned RL (GCRL) extends the RL framework to a multi-goal setting $(\mathcal{S} \times \mathcal{G}, \mathcal{A}, p, p_0, p_{\mathcal{G}}, r_{\mathcal{G}})$, where \mathcal{G} is the goal space, eg positions to reach, $r_{\mathcal{G}} : \mathcal{S} \times \mathcal{A} \times \mathcal{G} \rightarrow \mathbb{R}$ the new reward function, and $p_{\mathcal{G}} \in \mathcal{P}(\mathcal{G})$ the distribution of goals sampled at the beginning of each episode. In this setting, we consider a goal-conditioned (GC) policy $\pi : \mathcal{S} \times \mathcal{G} \rightarrow \mathcal{P}(\mathcal{A})$ whose objective is to maximize $\mathbb{E}_{g \sim p_{\mathcal{G}}, \pi(\cdot, \cdot, g)} \left[\sum_{t=0}^{+\infty} \gamma^t r_{\mathcal{G}}(s_t, a_t, g) \right]$, so that the resulting policy maximizes goal space coverage [31]. In our framework, we consider a sparse reward setting, where the reward is equal to 1 when the goal g is reached and 0 otherwise. It avoids the need for complicated reward engineering but requires relabelling to learn from failed attempts. We use Hindsight Experience Replay (HER) with "future" strategy combined with SAC for policy learning [6, 18].

3.3 Safe Reinforcement Learning

Safe RL aims at solving an RL problem under constraints, summarized in a Constrained MDP (CMDP) $(\mathcal{S}, \mathcal{A}, p, p_0, r_S, h)$, where $h : \mathcal{S} \rightarrow \mathbb{R}$ is the constraint function [2]. In many safe RL algorithms h plays the same role as a reward function and the constraint is based on the expected sum of discounted costs (Cf section 2). As the sum form allows compensations between terms, it does not guarantee that every state s in an episode verifies $h(s) \leq 0$. Therefore, we rather opted for the RCRL framework and its reachability critic that offer such a guarantee [40]. Also, it relates the reachability value to a notion of distance between the current state and the set of unsafe states, which is a crucial aspect of our action selection mechanism.

3.4 Distributional Reinforcement Learning

Safe exploration is inherently related to a notion of risk. To explore the agent has to go through previously unvisited states. But to do so it must already have some *a priori* knowledge about the safety of the states it is about to visit. A balancing robot for example may have to evaluate the probability to fall given its current state s and the action a it is about to execute. Distributional RL methods based on quantile regression, like TQC, allow to compute such a probability [11, 24]. Rather than computing the mean of the return distribution, their critic function approximates the entire distribution using a sum of Dirac delta functions $Z_\psi(s, a) := \frac{1}{N} \sum_{i=1}^N \delta_{\theta_\psi^{(i)}(s, a)}$. Each Dirac position $\theta_\psi^{(i)}(s, a)$ corresponds to a quantile of the return distribution, and N is the number of quantiles. Parameter ψ is optimized via quantile regression Q-learning [11] updates on batches of transitions uniformly sampled from a replay buffer \mathcal{B} . The mean of all quantiles is the expected return $\mathbb{E} \left[\sum_{t=0}^{+\infty} \gamma^t r_S(s_t, a_t) \mid s, a \right]$ and we use it for policy learning.

By definition, each quantile $\theta_\psi^{(i)}(s, a)$ is associated to a cumulative probability $\hat{\tau}_i \triangleq \mathbb{P} \left(Z^\pi(s, a) \leq \theta_\psi^{(i)}(s, a) \right) = \frac{2i-1}{2N}$, with $i \in \{1, \dots, N\}$ [11]. We assume that the sum of rewards must not fall

below a given threshold v , which is associated to a potential mistake. As the cumulative distribution function is non-decreasing, if $\theta_\psi^{(i)}(s, a) \leq v$, then $\hat{\tau}_i = \frac{2i-1}{2N} \leq \mathbb{P} (Z^\pi(s, a) \leq v)$. As a result, the relative positions of the quantiles with respect to a given threshold allow us to master the risk level during the safe exploration phase of our method. In our implementation, for a given hyperparameter $\tau \in [0, 1]$, we compute the mean of quantiles $\theta_\psi^{(i)}(s, a)$ that verify $\hat{\tau}_i \leq \tau$, then we compare it to the threshold v to decide whether switching to the safety policy is necessary. For example, $\tau = 0.1$ corresponds to the worst 10% of possible value outcomes.

4 METHOD

In this section, we formalize the safe exploration problem and detail the method we propose to solve it.

4.1 Defining the safe exploration problem

We aim for our agent to learn how to maximize coverage of a goal set, which corresponds to solving a multi-goal MDP (section 3.2). However, the agent must also explore its environment safely, avoiding mistakes. In our framework, a mistake occurs when a terminal state is reached. Therefore, the agent must avoid terminal states during exploration. To do so, we provide our agent with a safety policy that we can activate when the GC policy is about to make a mistake and lead the agent out of danger.

A way to build this safety policy is under the angle of classic RL. We consider a set $N_0 \subset \mathcal{S}$ of states that are desirable in terms of safety, for instance near some equilibrium point. The safety reward r_S equals 1 if $s \in N_0$ and 0 otherwise. This reward setting is convenient as it relates the sum of rewards to the number of steps $T^{\pi\phi_S}(s, a)$ necessary to reach N_0 from a given state-action couple (s, a) . Then, to decide when to switch from one policy to the other we can compare the estimation given by the safety critic of the number of steps necessary to reach N_0 to a threshold.

However, critics are neural networks, which are continuous functions, while the number of steps is finite for states from which we can reach N_0 and infinite for terminal states regarding an optimal safety policy. Thus, it pushes the critic to generalize safety to unsafe states and leads the agent to believe that it can still use the GC policy even though objectively, it is about to make a mistake. Therefore, in addition to the temporal distance, we added a notion of distance in the state space between the current state and the set of terminal states. To do so, we assume the agent receives a cost value $h(s)$ at each environment step, where s is the current state and $h : \mathcal{S} \rightarrow \mathbb{R}$ a continuous constraint function that verifies $h(s) > 0$ if and only if s is a terminal state. In our framework, we identify terminal states as mistakes the agent absolutely has to avoid. Like in RCRL, the function h is related to a kind of distance between the current state s and the set of terminal states [40]. Assuming to have access to such a function is not very restrictive as robots have sensors and often state estimation modules. The continuity of function h is crucial as it allows for generalization from known states to unseen states. Indeed, an unvisited state near another visited and safe state which is far enough from terminal states is likely to be safe too. On the contrary, states near unsafe states are likely to be unsafe. As

a result, we switch from the GC policy to the safety policy if the number of steps to reach N_0 is too high or if $h(s)$ is close to 0.

All these considerations lead us to define the safe exploration problem as the combination of a CMDP $(\mathcal{S}, \mathcal{A}, p, p_0, r_S, h)$ and a multi-goal MDP $(\mathcal{S} \times \mathcal{G}, \mathcal{A}, p, p_0, p_G, r_G)$:

$$\mathcal{T} = (\mathcal{S} \times \mathcal{G}, \mathcal{A}, p, p_0, p_G, r_S, r_G, h) \quad (1)$$

In the pretraining phase, we train a parametrized stochastic safety policy π_{ϕ_S} that solves the CMDP. The CMDP is independent of the goal space as the notion of safety is independent of the goals pursued by the agent. We assume that we have access to simulation to perform the safety pretraining, allowing us to perform reset anywhere and then to train the policy on a wide variety of situations. The critics that have been trained are then used in the action selection mechanism.

During the safe exploration phase, the safety policy and its critics are fixed and we train a GC policy. The multi-goal MDP part follows the framework developed in section 3.2. Transitions are collected and stored in an episodic replay buffer \mathcal{B} , regardless of the policy that generates them. Thus transitions generated by both policies can be found in the same episode. The main idea behind is that both policies can learn from each other as their respective objectives may be complementary in some situations.

4.2 Safety policy learning

To train the safety policy, we take inspiration from the distributional algorithm TQC, as it uses an ensemble critics for robustness and truncation in the critic update to prevent overestimation [24]. On the one hand, we train M approximations $Z_{\psi_1}, \dots, Z_{\psi_M}$ of the safety policy return distribution $Z^{\pi_{\phi_S}}(s, a) = \mathcal{D}\pi_{\phi_S} \left[\sum_{t=0}^{+\infty} \gamma^t r_S(s_t, a_t) \right] s, a$ using the TQC critic loss. The targets $Z_{\psi_1}, \dots, Z_{\psi_M}$ are initialized in the same way and follow $Z_{\psi_1}, \dots, Z_{\psi_M}$ via exponential moving average update. Similarly, we train an ensemble of M reachability critics $R_{\xi_1}, \dots, R_{\xi_M}$ but we replace the usual target based on a sum with the RCRL [40] target based on a max operator, leading to equation (2). Likewise, targets $R_{\xi_1}, \dots, R_{\xi_M}$ follow $R_{\xi_1}, \dots, R_{\xi_M}$ via exponential moving average. Unlike TQC, the reachability critics are updated separately using the quantile regression loss [11]. Critic ensemble are trained on the same batched transitions but initialized with different seeds.

$$\mathcal{T}\theta^{(j)} = (1 - \gamma)h(s') + \gamma \max \left(h(s'), \theta_{\xi}^{(j)}(s', a') \right) \quad (2)$$

Policy parameters ϕ_S are optimized to minimize the following loss, also inspired by TQC [24]:

$$\mathcal{L}_{\pi_S}(\phi_S) = \mathbb{E}_{s, a \sim \mathcal{B}} \left[\alpha \log \pi_{\phi_S}(a|s) - \bar{Q}(s, a) + \lambda \bar{R}(s, a) \right] \quad (3)$$

where $\bar{Q}(s, a) = \frac{1}{MN} \sum_{i=1}^M \sum_{j=1}^N \theta_{\psi_i}^{(j)}(s, a)$

$\bar{R}(s, a) = \frac{1}{MN} \sum_{i=1}^M \sum_{j=1}^N \theta_{\xi_i}^{(j)}(s, a)$ and $\lambda \in \mathbb{R}_+$ is a positive multiplier that we keep fixed. In our experiments, we performed an ablation study to identify the effect of reachability critics on safety during exploration. So we tested $\lambda = 0$ and $\lambda = 100$. The value of 100 has been chosen so that $\bar{Q}(s, a)$ and $\bar{R}(s, a)$ have the same scale.

We also tested a varying λ , like Ha et al., but it led to too much instability in the safety training [17].

4.3 Action selection mechanism

Algorithm 1 Action selection for safe exploration

- 1: **Inputs:** $s, g, \text{safety_flag}, \text{th}_{GC \rightarrow S}, \text{th}_{S \rightarrow GC}$
 - 2: $a_{GC} \sim \pi_{\phi_{GC}}(\cdot | s, g)$; $a_S \sim \pi_{\phi_S}(\cdot | s)$
 - 3: $\text{lower} \leftarrow (\hat{\sigma}^{\pi_{\phi_S}}(s, a_{GC}) > \text{th}_{S \rightarrow GC})$
 - 4: $\text{raise} \leftarrow (\hat{\sigma}^{\pi_{\phi_S}}(s, a_S) > \text{th}_{GC \rightarrow S})$
 - 5: $\text{safety_flag} \leftarrow \text{safety_flag} \text{ and } \text{lower}$ // Lower the flag
 - 6: $\text{safety_flag} \leftarrow \text{safety_flag} \text{ or } \text{raise}$ // Raise the flag
 - 7: $a \leftarrow \text{safety_flag} \cdot a_S + (1 - \text{safety_flag}) \cdot a_{GC}$
 - 8: **Return** $a, \text{safety_flag}$
-

The action selection mechanism that must ensure safe exploration has been reproduced in Algorithm 1. It takes as input the current state s , current desired goal g , the current value of a boolean flag, called `safety_flag`, and risk thresholds $\text{th}_{GC \rightarrow S}$ and $\text{th}_{S \rightarrow GC}$. The flag indicates which action to choose, and the role of the action selection mechanism is to update this flag. If equal to 1, action a_S sampled by the safety policy is selected, else action a_{GC} sampled by the GC policy is selected. The flag is updated according to the level of risk associated with state s and possible actions a_{GC} and a_S . If the level of risk $\hat{\sigma}^{\pi_{\phi_S}}(s, a_S)$ associated with state s and action a_S exceeds threshold $\text{th}_{GC \rightarrow S}$, the safety flag is set to 1 (*raised*) so as to avoid a future potentially dangerous situation. On the contrary, if the level of risk $\hat{\sigma}^{\pi_{\phi_S}}(s, a_{GC})$ associated with state s and action a_{GC} goes below threshold $\text{th}_{S \rightarrow GC}$, the safety flag is set to 0 (*lowered*). Note that the risk function $\hat{\sigma}^{\pi_{\phi_S}}$ is related to the safety policy, as its goal is to evaluate the capacity of the safety policy to put the agent out of danger. Also, because the safety policy is optimized on its critics, it tends to minimize the risk function indirectly. As a result, the thresholds should verify $\text{th}_{S \rightarrow GC} \leq \text{th}_{GC \rightarrow S}$. Otherwise, the safety policy would be the only one to act. Depending on the environment, one could choose either equality or strict inequality between thresholds (See section 5.3.1).

The framework defined in section section 4.1 essentially leads to two definitions of the risk function, leading to three different strategies. The first is based on the time necessary to reach the set N_0 from current state, using the safety policy. The second is based on the maximum of constraint function h along future trajectories generated by the safety policy. The third possibility is to combine both. We will use the labels **Time**, **Constraint** and **Time-constraint** for the respective three strategies.

Time: We choose the set N_0 so that, if the safety policy is well trained, then N_0 is a forward set regarding the safety policy π_{ϕ_S} . More precisely, we assume that, for any sequence of transitions $(s_0, a_0, \dots, s_t, \dots)$ generated by π_{ϕ_S} , if the starting state s_0 lies in N_0 , then all future states s_t also lie in N_0 . Under this assumption the safety reward $r_S(s_t, a_t)$ equals 0 until s_t lies in N_0 , resulting in equation (4):

$$T^{\pi_{\phi_S}}(s_0, a_0) = f_{\gamma} \left(\sum_{t=0}^{+\infty} \gamma^t r_S(s_t, a_t) \right) \quad (4)$$

where $T^{\pi\phi_S}(s_0, a_0)$ is the random variable corresponding to the number of steps necessary for π_{ϕ_S} to reach N_0 starting from state-action couple (s_0, a_0) , and $f_\gamma(x) = \log((1-\gamma)x) / \log \gamma$, which is a continuous bijection from $]0, 1/(1-\gamma)]$ to \mathbb{R}^+ . By applying the bijective mapping $f_\gamma(x)$ to the atoms $\theta_{\psi_i}^{(j)}(s, a)$ of ensemble $Z_{\psi_1}, \dots, Z_{\psi_M}$, we obtain new atoms that approximate the distribution of the random variable $T^{\pi\phi_S}(s, a)$. We denote $\hat{T}^{\pi\phi_S}(s, a; \tau)$ the mean of the quantiles corresponding to cumulative probabilities greater than τ . For example, $\tau = 0.9$ corresponds to the mean of worst 10% of cases. τ is a hyperparameter of the algorithm. In the Time strategy : $\hat{\sigma}^{\pi\phi_S}(s, a) = \hat{T}^{\pi\phi_S}(s, a; \tau)$. So the thresholds $\text{th}_{GC \rightarrow S}$ and $\text{th}_{S \rightarrow GC}$ are given in number of environment steps.

Constraint: In the same way, we denote $\hat{R}^{\pi\phi_S}(s, a; \tau)$ the mean of atoms from reachability critics $R_{\xi_1}, \dots, R_{\xi_M}$ corresponding to cumulative probabilities greater than τ . In the constraint strategy : $\hat{\sigma}^{\pi\phi_S}(s, a) = \hat{R}^{\pi\phi_S}(s, a; \tau)$. So the thresholds $\text{th}_{GC \rightarrow S}$ and $\text{th}_{S \rightarrow GC}$ are negative real numbers corresponding to safety margins.

Time-constraint: This strategy combines the two previous ones. Let $\epsilon > 0$ be a positive real number representing a safety margin. If $\hat{R}^{\pi\phi_S}(s, a; \tau) > -\epsilon$, then: $\hat{\sigma}^{\pi\phi_S}(s, a) = T_{max}$. Where T_{max} is the maximum number of episode steps. Otherwise: $\hat{\sigma}^{\pi\phi_S}(s, a) = \hat{T}^{\pi\phi_S}(s, a; \tau)$. The thresholds $\text{th}_{GC \rightarrow S}$ and $\text{th}_{S \rightarrow GC}$ are given in number of environment steps.

4.4 Algorithm

Pretraining phase: We use the same training loop as TQC [24]. The only difference is the gradient step update where, in addition to the TQC update, parameters ξ_1, \dots, ξ_M are updated by performing Adam optimizer step on loss \mathcal{L}_Z with target (2), and the actor loss is replaced with loss \mathcal{L}_{π_S} . Algorithm 2 describes how the update is done. The safety policy interacts with the environment, generating a transition that is stored in a replay buffer \mathcal{B}_S . Then a batch of transitions is sampled uniformly from the buffer and a gradient step update is performed on all parameters, so that for each stored transition, one step of gradient is performed. Also, we start the training after 5000 steps for which we sample random actions to favor exploration and learning at the start.

Algorithm 2 Safety gradient step update

- 1: Sample a batch from the replay buffer \mathcal{B}_S uniformly
 - 2: Perform TQC critic update on ψ_1, \dots, ψ_M [24]
 - 3: Update ξ_1, \dots, ξ_M using Adam on loss \mathcal{L}_Z with target (2)
 - 4: Update actor parameters ϕ_S using Adam on loss \mathcal{L}_{π_S}
 - 5: Update temperature α_S according to SAC rule [18]
-

Safe exploration phase: The procedure is summarized in Algorithm 3, which is also off-policy. We first choose safety thresholds depending on the risk level we want. Then the parameters of the previously learned safety policy and its critics are loaded, while the parameters related to the GC policy are randomly initialized. The episodic replay buffer is initially empty. For each environment step during training, the action selected according to Algorithm 1 to ensure safety during exploration. Each transition is stored in an episodic replay buffer \mathcal{B} regardless of the policy that generated it.

As a result, in a single stored episode, there are probably samples generated by both policies.

Initially, the GC policy performs poorly, as it has not yet been trained. Thus the first stored episodes contain a large majority of transitions generated by the safety policy, as it had to make up for the random behavior of the GC policy. Then, as the GC policy improves itself, the proportion of transitions it has generated increases in the buffer. The fact that many transitions have not been generated by the GC policy can lead off-policy algorithms like SAC to value over-estimation, due to the distributional drift between the dataset and the current learned policy [26]. This is why we used SAC-N instead of SAC, which is the same algorithm as SAC but with N critics instead of 2 [4]. As the critics are initialized and updated separately, disagreement between them regarding unvisited states is likely to lead the Bellman target to low values via the min operator, thus preventing over-estimation.

Algorithm 3 Safe exploration algorithm

- 1: **Inputs:** $\text{th}_{GC \rightarrow S}, \text{th}_{S \rightarrow GC}$
 - 2: **Load** Safety parameters $\psi_i, \bar{\psi}_i, \xi_i, \bar{\xi}_i, i \in \llbracket 1, M \rrbracket, \phi_S, \alpha_S$
 - 3: **Initialize** GC parameters $\psi_{GC}, \bar{\psi}_{GC}, \phi_{GC}, \alpha_{GC}$
 - 4: **Initialize** Episodic replay buffer $\mathcal{B} \leftarrow \emptyset$
 - 5: **Sample** initial state $s_0 \sim p_0$, and goal $g \sim p_G$
 - 6: **for** each iteration **do**
 - 7: **for** each environment step, until done **do**
 - 8: $a_t, \text{safety_flag} \leftarrow \text{select_action}(s, g, \text{safety_flag}, \text{th}_{GC \rightarrow S}, \text{th}_{S \rightarrow GC})$ (Algorithm 1)
 - 9: Collect transition $(s_t, a_t, s_{t+1}, r_{S,t}, r_{GC,t}, h_{t+1})$
 - 10: $\mathcal{B} \leftarrow \mathcal{B} \cup \{(s_t, a_t, s_{t+1}, r_{S,t}, r_{GC,t}, h_{t+1})\}$
 - 11: **end for**
 - 12: **for** each gradient step **do**
 - 13: Sample a batch $b_{GC} = (s_t, a_t, s_{t+1}, r_{GC,t})$ from \mathcal{B} using HER [6]
 - 14: Update GC parameters on b_{GC} using SAC-N rule [5]
 - 15: **end for**
 - 16: **end for**
 - 17: **return** GC parameters $\psi_{GC}, \bar{\psi}_{GC}, \phi_{GC}, \alpha_{GC}$
-

5 EXPERIMENTS

To appreciate the performance of our method, we conducted experiments on two environments: a custom goal-based version of the gymnasium CartPole environment [35] with continuous actions that we call *CartPoleGC*, and a goal environment based on the Skydio X2 drone from the Mujoco menagerie [41] that we call *SkydioX2GC*. We performed an ablation study to validate our design choices and compared our approach with the state-of-the-art GC method SAC + HER. Finally, as our general objective is zero error during exploration, we analyze the causes of the few mistakes we obtained during safe exploration for the best strategy.

5.1 Experimental setup

CartPoleGC and SkydioX2GC are interesting environments due to their inherent instability as random actions or even actions near 0 lead to mistakes.

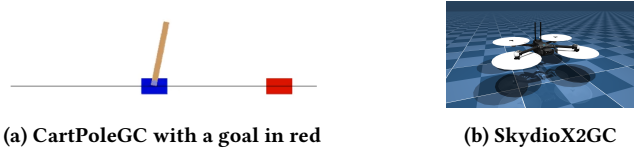


Figure 2: Environments

5.1.1 CartPoleGC. The state $s = (x, \dot{x}, \theta, \dot{\theta}) \in \mathcal{S}$ contains the position x of the cart, its velocity \dot{x} , the angle of the pole θ , and its velocity $\dot{\theta}$. x lies in $[-2.4m, 2.4m]$, and θ in $[-0.41rad, 0.41rad]$. Getting out of these bounds is considered a mistake, leading to episode termination. Action $a \in \mathcal{A} = [-1, 1]$ is proportional to the lateral force applied to the cart. 1 corresponds to 1 in the original discrete version and -1 to 0. Goals are desired positions of the cart: $\mathcal{G} = [-2.16, 2.16]$, sampled uniformly. The agent gets a goal reward when the cart is less than $0.05m$ near the the desired goal. The agent gets a safety reward when the x position lies in $[-2.2, 2.2]$ and other state variables in $[-0.05, 0.05]$, so $N_0 = [-2.2, 2.2] \times [-0.05, 0.05]^3$.

5.1.2 Skydio X2. The system physics is fully characterized by position (x, y, z) of the center of gravity, orientation (quaternions), linear velocity $(\dot{x}, \dot{y}, \dot{z})$ and angular velocity (Euler angles). The state is the concatenation of these elements. The (x, y) position lies in $[-3m, 3m]^2$, altitude z in $(1m, 4m)$, while roll and pitch angles are bounded to 30 deg of amplitude around 0. Getting out of these bounds is considered a mistake, leading to episode termination. The action space $\mathcal{A} = [-1, 1]^4$ corresponds to the forces applied on the rotors. Goals are desired (x, y, z) positions in the cube $[-2.6m, 2.6m] \times [-2.6m, 2.6m] \times [1.4m, 3.6m]$, sampled uniformly. The agent gets a goal reward when its less than $0.25m$ near the goal, and a safety reward when it is in the cube $N_0 = [-2.8m, 2.8m] \times [-2.8m, 2.8m] \times [1.2m, 3.8m]$.

Function h has the same structure in both environments. For a bounded state variable, eg x for CartPoleGC, corresponds a function h_x , computed according to equation (5).

$$h_x(x) = \max\{-1 - 2 \frac{x - x_{middle}}{x_{max} - x_{min}}, 2 \frac{x - x_{middle}}{x_{max} - x_{min}} - 1\} \quad (5)$$

where $x_{middle} = (x_{max} + x_{min})/2$. The constraint value $h(s)$ is the maximum over all bounded state variables. The advantage of such a formulation is that h_x is bounded in $[-1.0, 0.]$, so that $\lambda \bar{R}^{\pi\phi_s}$ and $\bar{Q}^{\pi\phi_s}$ have the same scale (Cf section 4.2). Finally, for both environments, an episode is terminated when $h(s) > 0$ and truncated when the number of steps exceeds 500. Note that achieving a goal is not terminal. Thus the GC policy can be aggressive to reach the goal and maintain safety once the goal is reached. For both environments, reset anywhere is performed in pretraining, while in safe exploration a noisy reset centered on a single state is applied.

5.1.3 Baseline. For each environment, we compared our best safe exploration variant in terms of safety with the combination of SAC and HER (SAC + HER), with 80% of relabelling and *future* strategy, in terms of success rate and occurrence of mistakes [6, 18].

5.1.4 Comparisons settings. We trained safe exploration variants and the baseline 12 times with CartPoleGC and 9 times with SkydioX2GC. We performed fewer runs on SkydioX2GC because of

the computational cost. To obtain the 12 runs on CartPoleGC, we performed 4 pretrainings using 4 different seeds. Then, for each of these pre-trained safety policies, we trained 3 safe exploring agents with 3 seeds. The idea behind this is to avoid cherry picking and draw a fair comparison between algorithms as the quality of safe exploration strongly depends on the the pretraining. In the same way, we performed 3 pretrainings on Skydio with 3 different seeds and 3 safe explorations for each pretraining seed. Each pretraining takes 2 million steps for CartPoleGC and 2.5 million steps for SkydioX2GC. For safe exploration, it takes respectively 500 000 and 1 million steps. We are interested in minimizing the occurrence of mistakes for the worst possible run of each tested variant. So we show the mean, the minimum, and the maximum in our plots of mistake occurrence. As for the success rate, we show the mean and the standard deviation. In all our experiments we set $\tau = 0.9$, considering the 10% worst cases to compute the risk measure, and a margin $\epsilon = 0.1$ (Cf section 4.3).

5.2 Comparison with the baseline

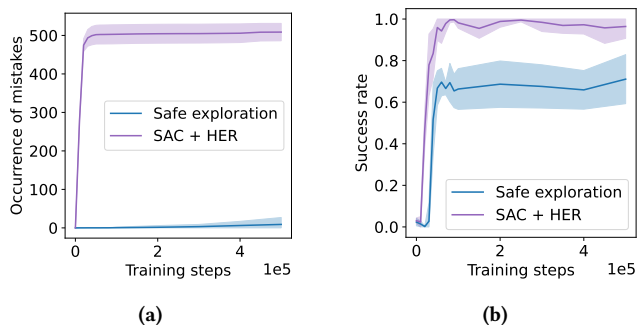


Figure 3: Comparison between our method (Cf L&S in section 5.3.1) and the baseline on the CartPoleGC environment in terms of safety during exploration and coverage.

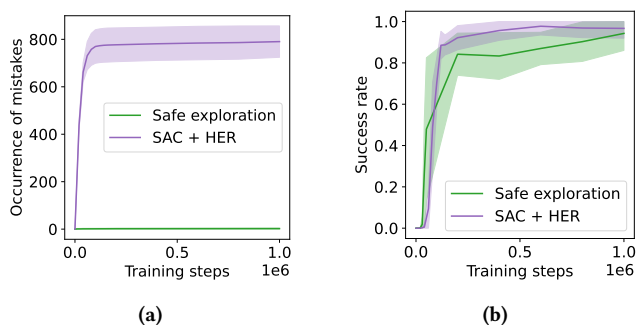


Figure 4: Comparison between our method (Cf S in section 5.3.1) and the baseline on the SkydioX2GC environment in terms of safety during exploration and coverage.

For both environments, we show that our approach can considerably reduce the number of mistakes during exploration in comparison to the baseline, as it does not take safety into account

(Figures 3 and 4). However, the baseline obtains a better success rate, around 98% on average against 70% for CartPoleGC (Figure 3b) while on SkydioX2GC safe exploration offers almost the same performance in coverage but with higher variance (Figure 4b). CartPoleGC’s poorer coverage can be explained by the fact that some goals are near terminal states so the policy prevents the cart from reaching it. We leave a coverage map in the supplementary material. Most importantly, we want to stress the minimum and maximum performance regarding safety. With CartPoleGC we obtained at most 27 mistakes, and with 7 mistakes SkydioX2GC, but for some runs, we obtained 0 mistakes for the whole training. As shown in section 5.4, these differences correspond to different pre-trained safety policies.

5.3 Ablation study

5.3.1 Effect of the reachability critics. In section 4.3, we describe three strategies to compute the risk function: Time, Constraint, and Time-constraint, that we would like to rate in terms of safety during exploration and coverage. Also, the λ factor used in pretraining can be set to 0 or 100 to take reachability critics into account or not in the actor update. The constraint (only) strategy led to catastrophic results in our preliminary experiments, both for learning and action selection, so we left it in the supplementary material. Four classes remain: *L&S* (reachability is taken into account both in safety learning and action selection), *L* (learning only), *S* (action selection only), *None* (reachability is not taken into account).

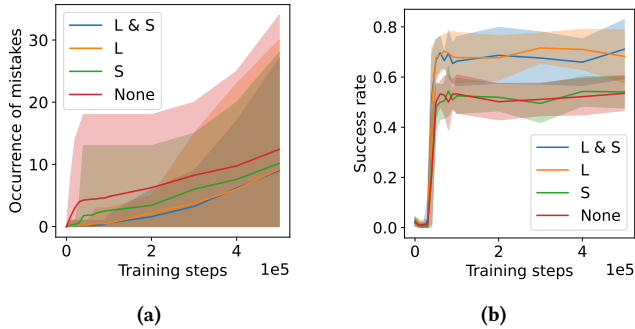


Figure 5: Effect of the reachability critics on safe exploration with CartPoleGC for different variants. *L&S* (reachability in safety learning and action selection), *L* (learning only), *S* (action selection only), *None* (no reachability)

First, it is interesting to note the difference between the two environments. In the case of CartPoleGC, the *L&S* combination is the best as it obtains the least mistakes (Figure 5a) with the highest coverage (Figure 5b). *S* obtains the least number of mistakes for SkydioX2GC (Figure 6a) while it performs poorly on CartPoleGC both in safety and coverage Figure 5. Also, while *L* offers the second-best safety performance for CartPoleGC, it obtains the worst safety performance with SkydioX2GC. Eventually, as *L&S* obtains a maximum of 10 mistakes against 7 for *S* and clearly outperforms *S* in terms of coverage, it appears as the default choice for both environments. Also one may observe a common pattern in Figures 5 and 6. In both cases including the reachability critic in the actor

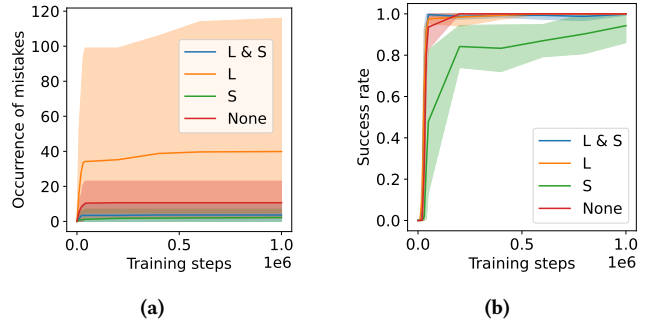


Figure 6: Effect of the reachability critics on safe exploration with SkydioX2GC for different variants. *L&S* (reachability in safety learning and action selection), *L* (learning only), *S* (action selection only), *None* (no reachability)

loss (*L* and *L&S*) leads to better coverage than other approaches. In the case of SkydioX2GC, we can see that other ablations than *S* perform way better in terms of coverage.

5.3.2 Effect of the thresholds and hysteresis. By construction, our method implies a tradeoff between safety during exploration and coverage. For instance, we remark that switching between the safety policy and the GC policy delays goal achievement in comparison to the full GC baseline. We leave videos in the supplementary material. Again, the results are very different between environments. As for CartPoleGC, we show that high thresholds (70 70 in Figure 7) lead to catastrophic performance in terms of safety during exploration, but also lead to better coverage. On the contrary low thresholds (30 30 in Figure 7) lead to zero safety violations for all seeds but also to very poor coverage. The best tradeoff between safety and coverage is obtained with $(th_{GC \rightarrow S}, th_{S \rightarrow GC}) = (70, 30)$, leading to a hysteresis behavior of the action selection mechanism. This choice was motivated by the fact that we have less confidence in the GC policy than in the safety policy to ensure safe exploration. As for SkydioX2GC, the result is the exact opposite. Equal thresholds lead to the best safety performance while the hysteresis choice seems to generate way more instability.

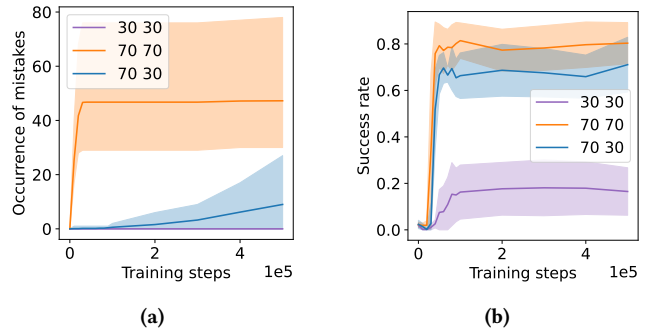


Figure 7: Effect of the thresholds on safe exploration with CartPoleGC for $(th_{GC \rightarrow S}, th_{S \rightarrow GC}) \in \{(30, 30), (70, 70), (70, 30)\}$ and the *L&S* variant.

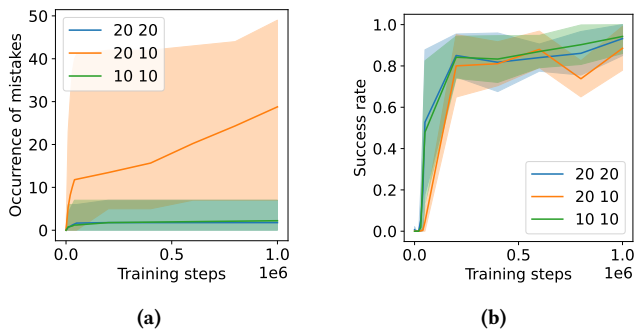
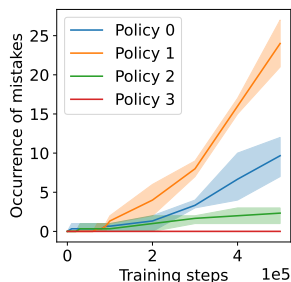


Figure 8: Effect of the thresholds on safe exploration with SkydioX2GC for $(th_{GC \rightarrow S}, th_{S \rightarrow GC}) \in \{(10, 10), (20, 20), (20, 10)\}$ and the S variant.

Figure 9: Occurrence of mistakes obtained during safe exploration for different pre-train policies with the Cart-PoleGC environment and $(th_{GC \rightarrow S}, th_{S \rightarrow GC}) = (70, 30)$



5.4 Analysing failure modes

In this section, we propose to analyze the causes of the few mistakes we obtained with our safe exploration method. Figure 9 shows that the result strongly depends on pretraining. For one safety policy (policy 3), we obtain zero mistakes over the 3 seeds of safe exploration training while we obtain more than 25 mistakes with the worst observed safety policy (policy 1). In order to avoid exhausting model selection engineering or cherry picking, we conducted a study to identify the failures' causes and obtain less variance with future algorithms. Although one could decide to reduce thresholds, we do not want to penalize coverage because of simplistic choices. Instead, we decided to analyse the trajectories stored in the episodic replay buffer \mathcal{B} that ended with a mistake to make a diagnosis. For CartpoleGC, with $(th_{GC \rightarrow S}, th_{S \rightarrow GC}) = (70, 30)$, all mistakes occur when the safety policy is active, meaning that the action selection mechanism has seen the danger and switched too late from the GC to the safety policy. Figure 10 shows a typical example of failure, characterized by a huge disagreement between critics before the mistake happens. This tends to show that the safety policy has not been trained a lot on the corresponding states and actions. It also offers two straightforward complementary perspectives of research. The first is to take disagreement into account in the switching mechanism. The second is to finetune the safety policy during the safe exploration phase to improve it, which is also confirmed by further analysis we left in the supplementary material.

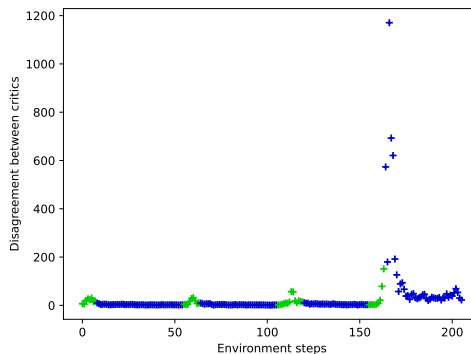


Figure 10: Critic disagreement in L_1 norm between the quantile critics of the same ensemble $Z^{\pi_{\phi_S}}$ along a failed episode of the CartPoleGC. Dots are green when the GC policy is activated and blue when the safety policy is activated.

6 CONCLUSION

Our experiments demonstrate that the safe exploration framework we developed successfully trains a goal-conditioned policy while preventing mistakes during learning. We showed that incorporating a notion of distance to terminal states is crucial for safety and examined the impact of thresholds on both safety and goal-space coverage. As zero error over the course of safe exploration is our objective, we analyzed failure modes to identify ways to reduce mistakes. The primary cause of failures lies in insufficient pretraining of the safety policy in certain regions of the state space. Improvements could be achieved by considering disagreement between critics as an intrinsic motivation during pretraining or incorporating it into the action selection mechanism. Additionally, fine-tuning the safety policy during the safe exploration phase could expand the set of reachable states, further enhancing exploration. Also, we will focus on improving the evaluation procedure of the safety policy. Our experiments reveal that the key is not only to have a safety policy we trust but also to have a clear understanding of its limitations.

REFERENCES

- [1] Joshua Achiam, David Held, Aviv Tamar, and Pieter Abbeel. 2017. Constrained policy optimization. In *International conference on machine learning*. PMLR, 22–31.
- [2] E. Altman. 1999. Constrained Markov Decision Processes.
- [3] Aaron D. Ames, Samuel Coogan, Magnus Egerstedt, Gennaro Notomista, Koushil Sreenath, and Paulo Tabuada. 2019. Control Barrier Functions: Theory and Applications. arXiv:1903.11199 [cs.SY]
- [4] Gaon An, Seungyong Moon, Jang-Hyun Kim, and Hyun Oh Song. 2021. Uncertainty-Based Offline Reinforcement Learning with Diversified Q-Ensemble. In *Advances in Neural Information Processing Systems*, M. Ranzato, A. Beygelzimer, Y. Dauphin, P.S. Liang, and J. Wortman Vaughan (Eds.), Vol. 34. Curran Associates, Inc., 7436–7447. https://proceedings.neurips.cc/paper_files/paper/2021/file/3d3d286a8d153a4a58156d0e02d8570c-Paper.pdf
- [5] Gaon An, Seungyong Moon, Jang-Hyun Kim, and Hyun Oh Song. 2021. Uncertainty-based offline reinforcement learning with diversified q-ensemble. *Advances in neural information processing systems* 34 (2021), 7436–7447.
- [6] Marcin Andrychowicz, Filip Wolski, Alex Ray, Jonas Schneider, Rachel Fong, Peter Welinder, Bob McGrew, Josh Tobin, OpenAI Pieter Abbeel, and Wojciech Zaremba. 2017. Hindsight Experience Replay. https://proceedings.neurips.cc/paper_files/paper/2017/file/453fadbd8a1a3af50a9df4df899537b5-Paper.pdf
- [7] Elliot Chane-Sane, Cordelia Schmid, and Ivan Laptev. 2021. Goal-conditioned reinforcement learning with imagined subgoals. In *International conference on*

- machine learning*. PMLR, 1430–1440.
- [8] Jongwook Choi, Archit Sharma, Honglak Lee, Sergey Levine, and Shixiang Shane Gu. 2021. Variational Empowerment as Representation Learning for Goal-Conditioned Reinforcement Learning. , 1953–1963 pages. <https://proceedings.mlr.press/v139/choi21b.html>
 - [9] Yinlam Chow, Ofir Nachum, Aleksandra Faust, Edgar Duenez-Guzman, and Mohammad Ghavamzadeh. 2019. Lyapunov-based Safe Policy Optimization for Continuous Control. arXiv:1901.10031 [cs.LG]
 - [10] Cédric Colas, Tristan Karch, Olivier Sigaud, and Pierre-Yves Oudeyer. 2022. Autotelic agents with intrinsically motivated goal-conditioned reinforcement learning: a short survey. *Journal of Artificial Intelligence Research* 74 (2022), 1159–1199.
 - [11] Will Dabney, Mark Rowland, Marc Bellemare, and Rémi Munos. 2018. Distributional Reinforcement Learning With Quantile Regression. <https://doi.org/10.1609/aaai.v32i1.11791>
 - [12] Gal Dalal, Krishnamurthy Dvijotham, Matej Vecerik, Todd Hester, Cosmin Paduraru, and Yuval Tassa. 2018. Safe Exploration in Continuous Action Spaces. arXiv:1801.08757 [cs.AI]
 - [13] Charles Dawson, Sicun Gao, and Chuchu Fan. 2022. Safe control with learned certificates: A survey of neural lyapunov, barrier, and contraction methods.
 - [14] Mehdi Fatemi, Shikhar Sharma, Harm Van Seijen, and Samira Ebrahimi Kahou. 2019. Dead-ends and Secure Exploration in Reinforcement Learning. In *Proceedings of the 36th International Conference on Machine Learning (Proceedings of Machine Learning Research, Vol. 97)*, Kamalika Chaudhuri and Ruslan Salakhutdinov (Eds.). PMLR, 1873–1881. <https://proceedings.mlr.press/v97/fatemi19a.html>
 - [15] Javier Garcia, Fern, and o Fernández. 2015. A Comprehensive Survey on Safe Reinforcement Learning. *Journal of Machine Learning Research* 16, 42 (2015), 1437–1480. <http://jmlr.org/papers/v16/garcia15a.html>
 - [16] J. Garcia and F. Fernandez. 2012. Safe Exploration of State and Action Spaces in Reinforcement Learning. *Journal of Artificial Intelligence Research* 45 (Dec. 2012), 515–564. <https://doi.org/10.1613/jair.3761>
 - [17] Sehoon Ha, Peng Xu, Zhenyu Tan, Sergey Levine, and Jie Tan. 2021. Learning to Walk in the Real World with Minimal Human Effort. , 1110–1120 pages. <https://proceedings.mlr.press/v155/ha21c.html>
 - [18] Tuomas Haarnoja, Aurick Zhou, Kristian Hartikainen, George Tucker, Sehoon Ha, Jie Tan, Vikash Kumar, Henry Zhu, Abhishek Gupta, Pieter Abbeel, and Sergey Levine. 2019. Soft Actor-Critic Algorithms and Applications. arXiv:1812.05905 [cs.LG]
 - [19] Nathan Hunt, Nathan Fulton, Sara Magliacane, Nghia Hoang, Subhro Das, and Armando Solar-Lezama. 2020. Verifiably Safe Exploration for End-to-End Reinforcement Learning. arXiv:2007.01223 [cs.AI] <https://arxiv.org/abs/2007.01223>
 - [20] Leslie Pack Kaelbling. 1993. Learning to Achieve Goals. <https://api.semanticscholar.org/CorpusID:5538688>
 - [21] Thommen George Karimpanal, Santu Rana, Sunil Gupta, Truyen Tran, and Svetha Venkatesh. 2020. Learning transferable domain priors for safe exploration in reinforcement learning. In *2020 International Joint Conference on Neural Networks (IJCNN)*. IEEE, 1–10.
 - [22] Sunin Kim, Jaewoon Kwon, Taeyoon Lee, Younghyo Park, and Julien Perez. 2023. Safety-Aware Unsupervised Skill Discovery. , 894-900 pages. <https://doi.org/10.1109/ICRA48891.2023.10160985>
 - [23] Torsten Koller, Felix Berkenkamp, Matteo Turchetta, Joschka Boedecker, and Andreas Krause. 2019. Learning-based Model Predictive Control for Safe Exploration and Reinforcement Learning. arXiv:1906.12189 [eess.SY] <https://arxiv.org/abs/1906.12189>
 - [24] Arsenii Kuznetsov, Pavel Shvechikov, Alexander Grishin, and Dmitry Vetrov. 2020. Controlling Overestimation Bias with Truncated Mixture of Continuous Distributional Quantile Critics. , 5556–5566 pages. <https://proceedings.mlr.press/v119/kuznetsov20a.html>
 - [25] Pawel Ladosz, Lilian Weng, Minwoo Kim, and Hyondong Oh. 2022. Exploration in deep reinforcement learning: A survey. *Information Fusion* 85 (Sept. 2022), 1–22. <https://doi.org/10.1016/j.inffus.2022.03.003>
 - [26] Sergey Levine, Aviral Kumar, George Tucker, and Justin Fu. 2020. Offline reinforcement learning: Tutorial, review, and perspectives on open problems. *arXiv preprint arXiv:2005.01643* (2020).
 - [27] Zachary C. Lipton, Kamyar Azizzadenesheli, Abhishek Kumar, Lihong Li, Jianfeng Gao, and Li Deng. 2018. Combating Reinforcement Learning’s Sisyphian Curse with Intrinsic Fear. arXiv:1611.01211 [cs.LG] <https://arxiv.org/abs/1611.01211>
 - [28] Soroush Nasiriany, Vitchyr H. Pong, Steven Lin, and Sergey Levine. 2019. Planning with Goal-Conditioned Policies. arXiv:1911.08453 [cs.LG] <https://arxiv.org/abs/1911.08453>
 - [29] Vitchyr H. Pong, Murtaza Dalal, Steven Lin, Ashvin Nair, Shikhar Bahl, and Sergey Levine. 2020. Skew-Fit: State-Covering Self-Supervised Reinforcement Learning. arXiv:1903.03698 [cs.LG] <https://arxiv.org/abs/1903.03698>
 - [30] William Saunders, Girish Sastry, Andreas Stuhlmüller, and Owain Evans. 2017. Trial without Error: Towards Safe Reinforcement Learning via Human Intervention. arXiv:1707.05173 [cs.AI] <https://arxiv.org/abs/1707.05173>
 - [31] Tom Schaul, Daniel Horgan, Karol Gregor, and David Silver. 2015. Universal Value Function Approximators. In *Proceedings of the 32nd International Conference on Machine Learning (Proceedings of Machine Learning Research, Vol. 37)*, Francis Bach and David Blei (Eds.). PMLR, Lille, France, 1312–1320. <https://proceedings.mlr.press/v37/schaul15.html>
 - [32] Krishnan Srinivasan, Benjamin Eysenbach, Sehoon Ha, Jie Tan, and Chelsea Finn. 2020. Learning to be Safe: Deep RL with a Safety Critic. arXiv:2010.14603 [cs.LG]
 - [33] Richard S. Sutton and Andrew G. Barto. 2018. Reinforcement Learning: An Introduction. <http://incompleteideas.net/book/the-book-2nd.html>
 - [34] Yichuan Charlie Tang, Jian Zhang, and Ruslan Salakhutdinov. 2019. Worst Cases Policy Gradients. arXiv:1911.03618 [cs.LG]
 - [35] Mark Towers, Ariel Kwiatkowski, Jordan Terry, John U Balis, Gianluca De Cola, Tristan Deleu, Manuel Goulão, Andreas Kallinteris, Markus Krimmel, Arjun KG, et al. 2024. Gymnasium: A Standard Interface for Reinforcement Learning Environments.
 - [36] Matteo Turchetta, Felix Berkenkamp, and Andreas Krause. 2016. Safe Exploration in Finite Markov Decision Processes with Gaussian Processes. arXiv:1606.04753 [cs.LG] <https://arxiv.org/abs/1606.04753>
 - [37] Akifumi Wachi, Wataru Hashimoto, Xun Shen, and Kazumune Hashimoto. 2024. Safe exploration in reinforcement learning: A generalized formulation and algorithms. *Advances in Neural Information Processing Systems* 36 (2024).
 - [38] Pierre-Brice Wieber. 2008. Viability and predictive control for safe locomotion. In *2008 IEEE/RSJ International Conference on Intelligent Robots and Systems*. 1103–1108. <https://doi.org/10.1109/IROS.2008.4651022>
 - [39] Qisong Yang, Thiago D. Simão, Simon H Tindemans, and Matthijs T. J. Spaan. 2021. WCSAC: Worst-Case Soft Actor Critic for Safety-Constrained Reinforcement Learning. <https://doi.org/10.1609/aaai.v35i12.17272>
 - [40] Dongjie Yu, Haitong Ma, Shengbo Li, and Jianyu Chen. 2022. Reachability Constrained Reinforcement Learning. , 25636–25655 pages. <https://proceedings.mlr.press/v162/yu22d.html>
 - [41] Kevin Zakka, Yuval Tassa, and MuJoCo Menagerie Contributors. 2022. MuJoCo Menagerie: A collection of high-quality simulation models for MuJoCo. http://github.com/google-deepmind/mujoco_menagerie

A SUPPLEMENTARY MATERIAL

A.1 Videos

- failure_cartpole.mp4: CartPoleGC failure mode described in the paper ($(th_{GC \rightarrow S}, th_{S \rightarrow GC}) = (70, 30)$).
- near_bound_cartpole.mp4: CartPoleGC with a "difficult" goal near the environment bounds, thus near unsafe states ($(th_{GC \rightarrow S}, th_{S \rightarrow GC}) = (70, 30)$).
- simple_cartpole.mp4: CartPoleGC with a simple goal with $(th_{GC \rightarrow S}, th_{S \rightarrow GC}) = (70, 30)$.
- 30_30_cartpole.mp4: CartPoleGC with a simple goal with $(th_{GC \rightarrow S}, th_{S \rightarrow GC}) = (30, 30)$ to show the impact of low thresholds on coverage.
- skydioX2_example.mp4: Example of SkydioX2 reaching a goal ($(th_{GC \rightarrow S}, th_{S \rightarrow GC}) = (10, 10)$)

Note that for CartPoleGC, the cart is blue when the safety policy is activated and green otherwise. The goal is represented by a red box.

A.2 Further analysis of failure modes

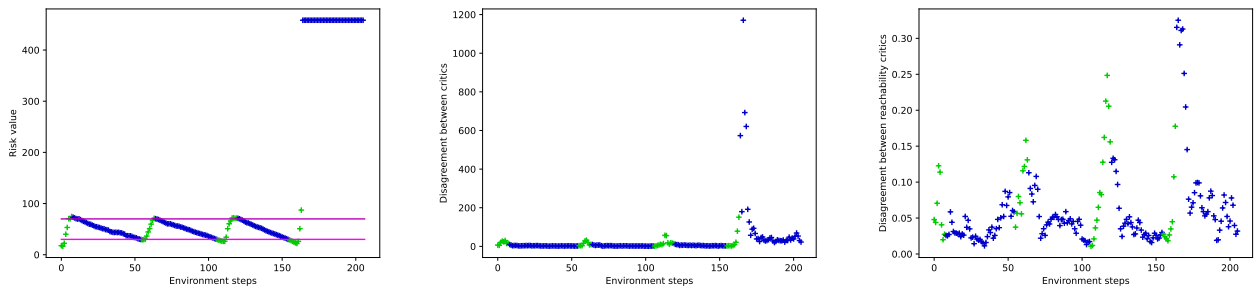


Figure 11: From left to right: Value of the risk function $\hat{\sigma}^{\pi\phi_S}(s, a)$ along the failed episode shown as an example in Figure 10, where the thresholds are represented in magenta and purple ; Critic disagreement (Figure 10) ; Reachability critic disagreement. Blue dots correspond to the safety policy and green dots to the GC policy. One can see the hysteretic behavior on the left plot. A video of the failure (failure_cartpole.mp4) is also attached.

We can see on the left plot (Figure 11) that the agent switches from the GC policy to the safety policy before making a mistake. We also observe that the oscillations of the disagreement, for both ensemble of critics, are synchronized with the change of policies. Indeed, as the GC policy has a different objective than the safety policy, it goes towards states that have been less visited by the safety policy during its pretraining. This phenomenon motivates safety finetuning for future works.

A.3 Goal-space coverage performance with safe exploration on CartPoleGC

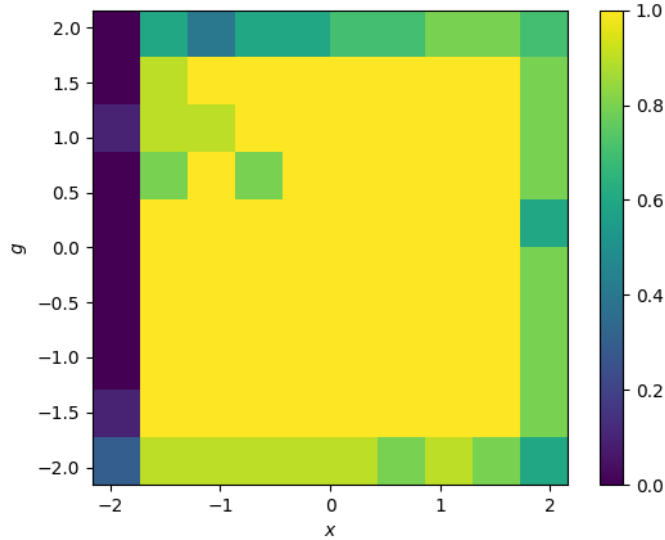


Figure 12: Coverage map obtained with *L&S* safe exploration variant and $(th_{GC \rightarrow S}, th_{S \rightarrow GC}) = (70, 30)$ on CartPoleGC. Only for this experience, the cartpole is reset on different x positions. Each cell corresponds to the combination of a starting position and a desired goal and we measure the success rate. We can see that the success rate is lower for starting positions and goals near the environment bounds, than for positions around the center. The safety policy tends to prevent the agent from reaching goals near the bounds. In the same way, if the initial state is too close to the bound, the safety policy prevents the GC policy from acting most of the time.

A.4 Constraint strategy

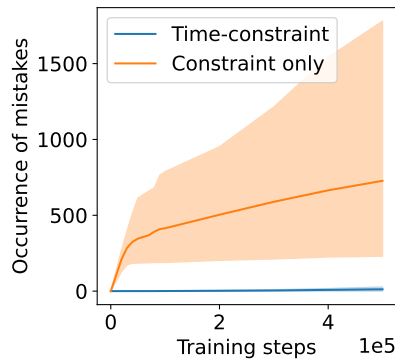


Figure 13: Occurrence of mistakes obtained with the time-constraint strategy and the constraint (only) strategy on the Cart-PoleGC environment. Performance of constraint strategy in terms of safety is catastrophic.

A.5 Agent hyperparameters

As for the buffer we choose to keep all transitions. There is no forgetting. Thus, the buffer size is always larger than the number of training steps.

Table 1: Safety pretraining: TQC’s hyperparameters

<i>Name</i>	<i>Value</i>
Actor learning rate	3×10^{-4}
Critic learning rate	3×10^{-4}
Temperature learning rate	3×10^{-4}
Initial temperature	1.0
τ	5×10^{-3}
No entropy backup	-
Discount factor	0.99
Hidden layers	(256, 256)
Number of critics	5
Number of atoms per critic	25
Number of quantiles to drop	2 for CartPoleGC ; 0 for SkydioX2GC

Table 2: Safety pretraining: Reachability critics’ hyperparameters

<i>Name</i>	<i>Value</i>
Critic learning rate	3×10^{-4}
τ	5×10^{-3}
Discount factor	0.99
Hidden layers	(256, 256)
Number of critics	5
Number of atoms per critic	25

Table 3: SAC and SAC-N hyperparameters for safe exploration

<i>Name</i>	<i>Value</i>
Actor learning rate	3×10^{-4}
Critic learning rate	3×10^{-4}
Temperature learning rate	3×10^{-4}
Initial temperature	1.0
τ	5×10^{-3}
No entropy backup	-
Discount factor	0.99
Hidden layers	(256, 256)
Number of critics (Specific to SAC-N)	50 for CartPoleGC ; 10 for SkydioX2GC